Supplemental Information

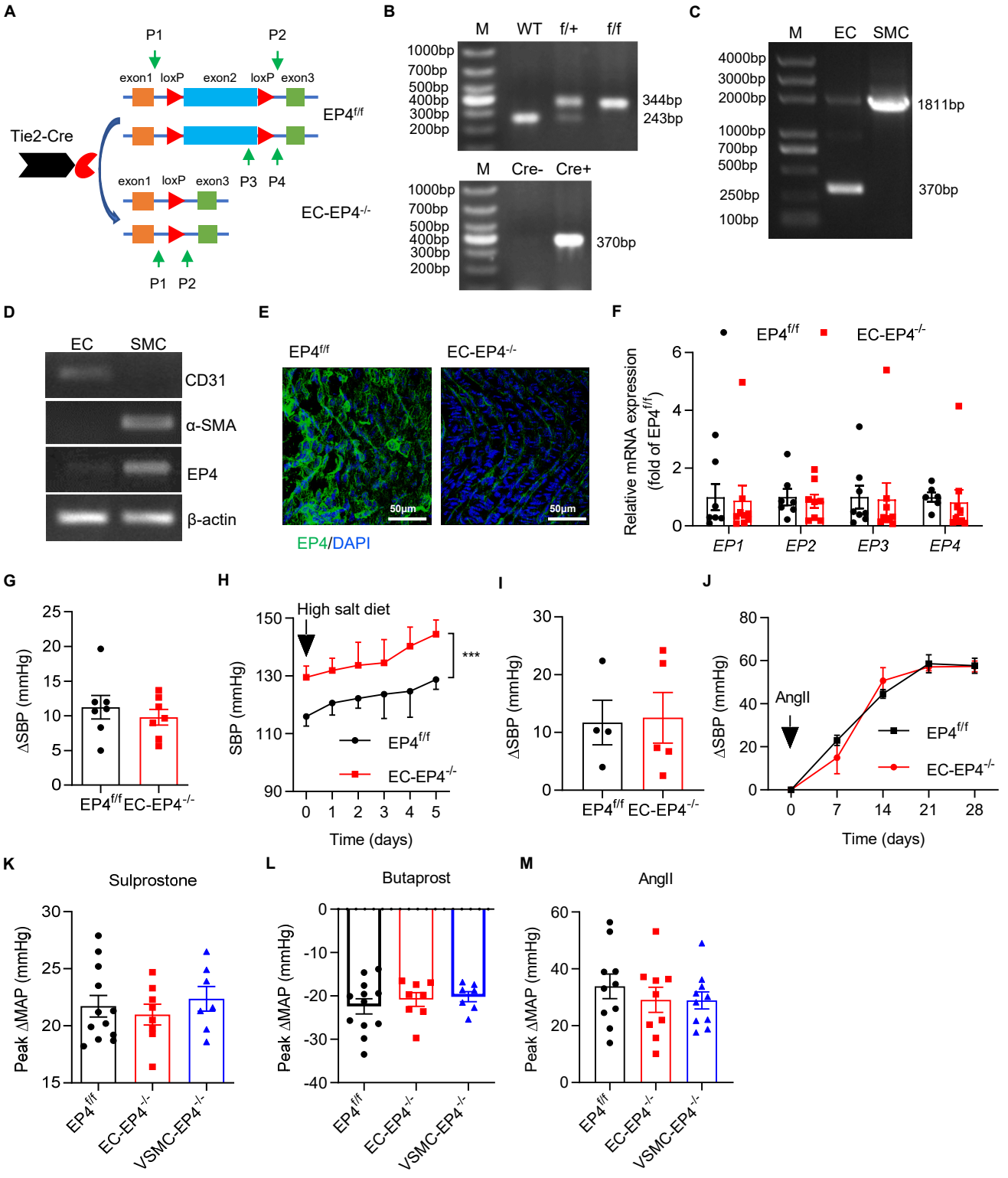

Figure S1. Genotype validation and blood pressure changes in the EC-EP4$^{-/-}$ mice under various treatments. (**A**) Schematic structure of the floxed EP4 allele (EP4$^{f/f}$) and Tie2-Cre-modified allele (EC-EP4$^{-/-}$). The locations of two loxP sites flanking the exon 2 of the EP4 gene are shown. The P1 and P2 are the primers designed to detect the presence or absence of the exon 2. The P3 and P4 are the primers designed to detect the 2nd loxP site. All primer sequences are shown in Table S4. (**B**) Validation of the wild type (WT), EP4$^{f/+}$ and EP4$^{f/f}$ alleles and Cre recombinase transgene by PCR using mouse tail DNA and the primer 3 (P3) and primer 4 (P4). The 243 bp

band and 344 bp band represents the WT allele and the floxed EP4 allele, respectively. The 370 bp band represents the cre transgene that presents only in the EC-EP4$^{-/-}$ mice. M: marker. (**C**) PCR analysis of the floxed EP4 allele (1,811 bp) or the EP4 allele with the exon 2 excised (370 bp) using DNA isolated from the aortic endothelium layer and smooth muscle layer of the EC-EP4$^{-/-}$ mouse using the primer 1 (P1) and primer 2 (P2). M: marker. EC: endothelial cell layer; SMC: smooth muscle cell layer. (**D**) RT-PCR assay demonstrating that the absence of EP4 mRNA in the EC and the presence of EP4 mRNA in the SMC of the EC-EP4$^{-/-}$ mouse. CD31 and α-SMA were used as positive controls for the EC and SMC, respectively. (**E**) *En face* immunofluorescence staining showing a significant reduction in EP4 protein expression in the aortic endothelium layer of the EC-EP4$^{-/-}$ mice. The green color represents the presence of the EP4 protein, while the blue shows the cell nuclei. Scale bars: 50 μm. (**F**) Real-time PCR analysis showing no change in mRNA levels of four EP receptors in the aortas of the EP4$^{f/f}$ and EC-EP4$^{-/-}$ mice. (**G**) The net changes of SBP in the EP4$^{f/f}$ and EC-EP4$^{-/-}$ mice after 2-week high-salt diet feeding. n=5-7. (**H** and **I**) Radiotelemetry measurement showing the time-course of the effect of high-salt diet on SBP in the EP4$^{f/f}$ and EC-EP4$^{-/-}$ mice (H). The net changes of SBP after 5-day high-salt diet feeding were compared between two genotypes (I). ***p<0.001 *vs.* EP4$^{f/f}$, n=5. **J.** Comparable net changes of SBP during Ang II infusion in the EP4$^{f/f}$ and EC-EP4$^{-/-}$ mice. n=11-14. (**K**-**M**) The maximal changes of MAP (Peak ∆MAP) after sulprostone (K), butaprost (L) and Ang II (L) infusion in the EP4$^{f/f}$, EC-EP4$^{-/-}$ and VSMC-EP4$^{-/-}$ mice. n=8-16. Data are represented as mean ± SEM, 2-tailed Student's t tests for **F**, **G** and **I**; 2-way ANOVA tests for **H** and **J**; 1-way ANOVA followed by Dunnett's multiple comparisons tests for **K**-**M**.

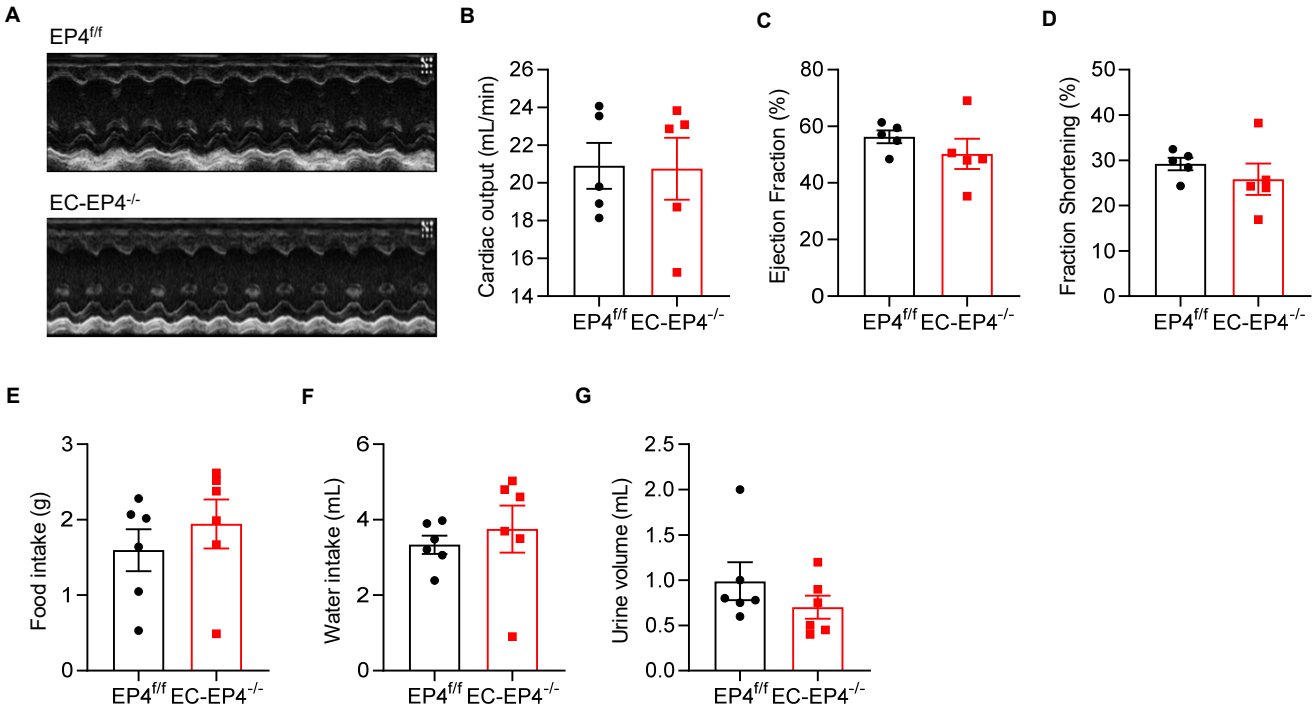

Figure S2. Cardiac functions, food and water intake and urine output of the EP4$^{f/f}$ and EC-EP4$^{-/-}$ mice. (A) Representative echocardiography images in the EP4$^{f/f}$ and EC-EP4$^{-/-}$ mice. **(B)** Comparison of cardiac output between EP4$^{f/f}$ and EC-EP4$^{-/-}$ mice. n=5. **(C)** Cardiac ejection fraction was similar in the EP4$^{f/f}$ and EC-EP4$^{-/-}$ mice. n=5. **(D)** Left ventricular shortening fractions were comparable in the EP4$^{f/f}$ and EC-EP4$^{-/-}$ mice. n=5. **(E-G)** Daily food intake (E), water consumption (F) and urine output (G) were similar in the EP4$^{f/f}$ and EC-EP4$^{-/-}$ mice, n=6-7. Data are represented as mean ± SEM, 2-tailed Student's t tests for **B-G**.

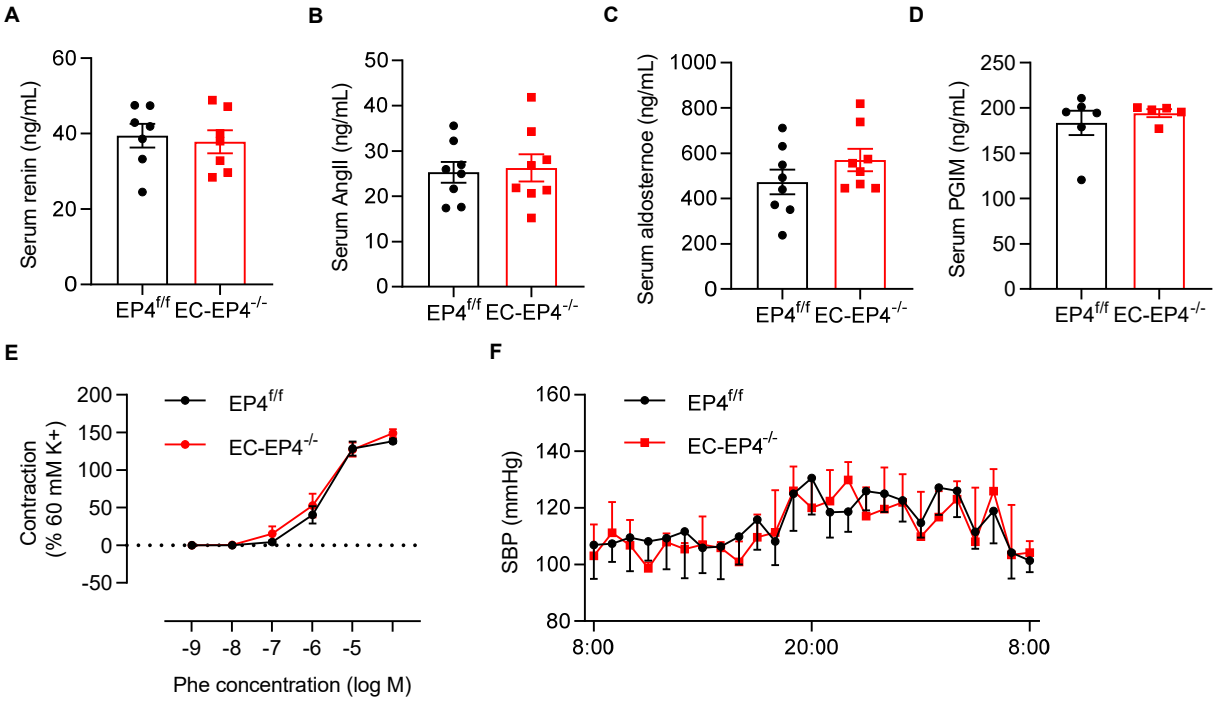

Figure S3. Effect of endothelial deletion of EP4 on the RAS system and vasoactive responses to phenylephrine and L-NAME. (**A-C**) No difference in serum renin (A), AngII (B) and aldosterone (C) levels was observed between the $EP4^{f/f}$ and $EC\text{-}EP4^{-/-}$ mice. n=6-7. (**D**) Serum levels of the PGI_2 metabolites (PGIM) were comparable in the $EP4^{f/f}$ and $EC\text{-}EP4^{-/-}$ mice. n=5-6. (**E**) No difference in phenylephrine (Phe)-evoked vasoconstriction of the mesenteric arterial rings between the $EP4^{f/f}$ and $EC\text{-}EP4^{-/-}$ mice. n=8. (**F**) Telemetry measurement showing that 2-week treatment of L-NAME abolished the difference of SBP between the $EP4^{f/f}$ and $EC\text{-}EP4^{-/-}$ mice. n=3. Data are represented as mean ± SEM, 2-tailed Student's t tests for **A-D**; 2-way ANOVA tests for **E** and **F**.

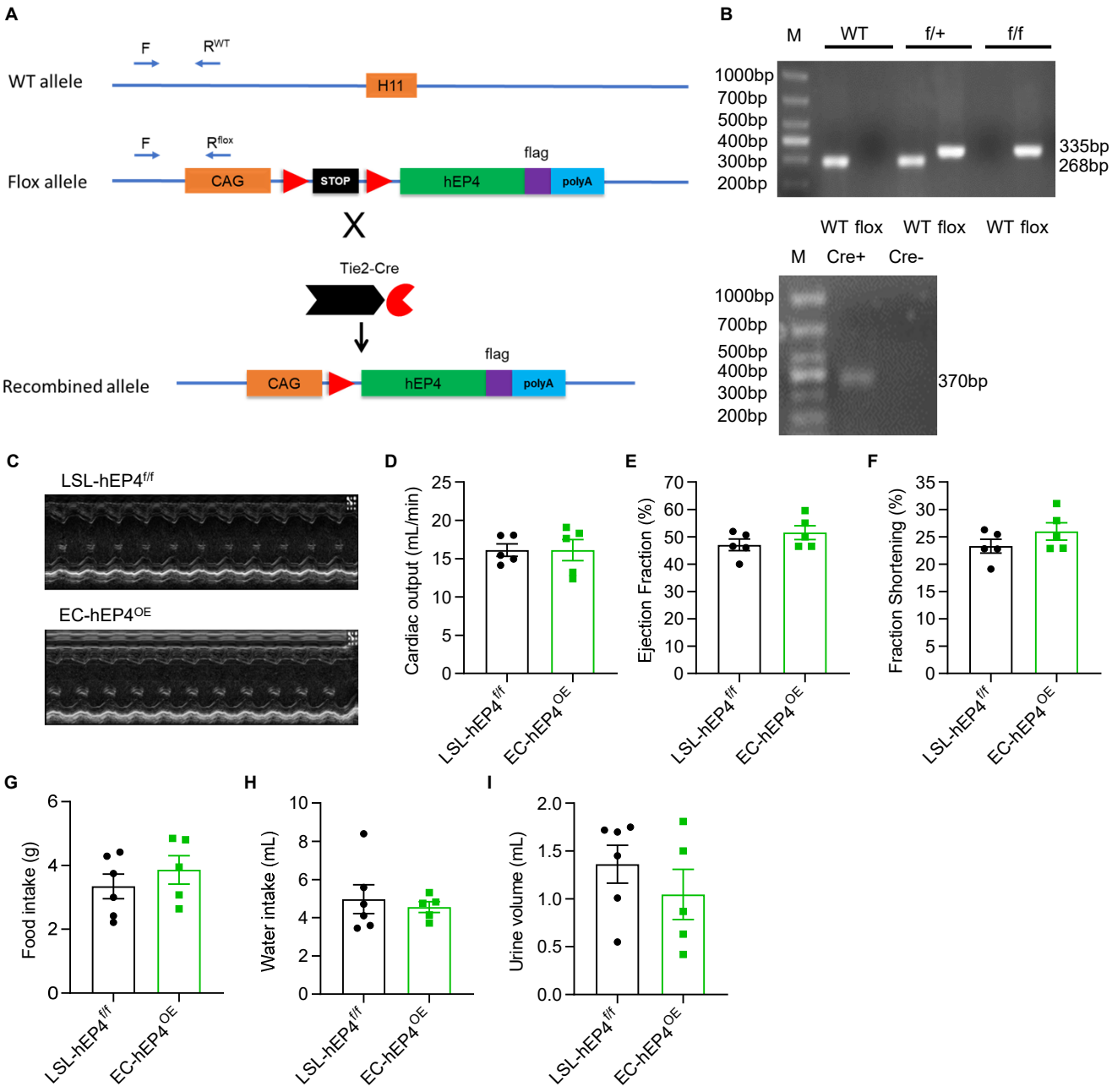

Figure S4. Generation of the EC-hEP4^{OE} mice and effect of endothelial overexpression of EP4 on cardiac and renal function. (**A**) Schematic diagram showing the H11-CAG-loxp-stop-loxp-hEP4 fragment inserted allele (LSL-hEP4$^{f/f}$) and Tie2-Cre recombinase modified allele. F: common forward primer, R^{WT}: reverse primer for the WT allele, R^{flox}: reverse primer for the floxed allele. All primer sequences are listed in Table S4. (**B**) PCR-based genotyping of the wild type (WT), LSL-hEP4$^{f/+}$, and LSL-hEP4$^{f/f}$ alleles and the Cre recombinase transgene using mouse tail DNA. The 268 bp band (using primer F and R^{WT}) represents the WT allele and the 335 bp band (using primer F and R^{flox}) represents the floxed allele. The 370 bp band represents the Cre transgene that presents only in the EC-hEP4^{OE} mice. M: molecular marker. (**C**) Representative echocardiography images in the LSL-hEP4$^{f/f}$ and EC-hEP4^{OE} mice. (**D**) Cardiac output was comparable in the LSL-hEP4$^{f/f}$ and EC-hEP4^{OE} mice. n=5. (**E**) Ejection fraction was indistinguishable in the LSL-hEP4$^{f/f}$ and EC-hEP4^{OE} mice. n=5. (**F**) No difference of left ventricular shortening fractions was observed between the EP4$^{f/f}$ and EC-EP4$^{-/-}$ mice. n=5. (**G-I**) Daily food consumption (G), water intake (H) and urine output (I) of the LSL-hEP4$^{f/f}$ and EC-hEP4^{OE} mice. n=5-6. Note: no difference was observed between two genotypes. Data are represented as mean ± SEM. 2-tailed Student's t tests for **D-I**.

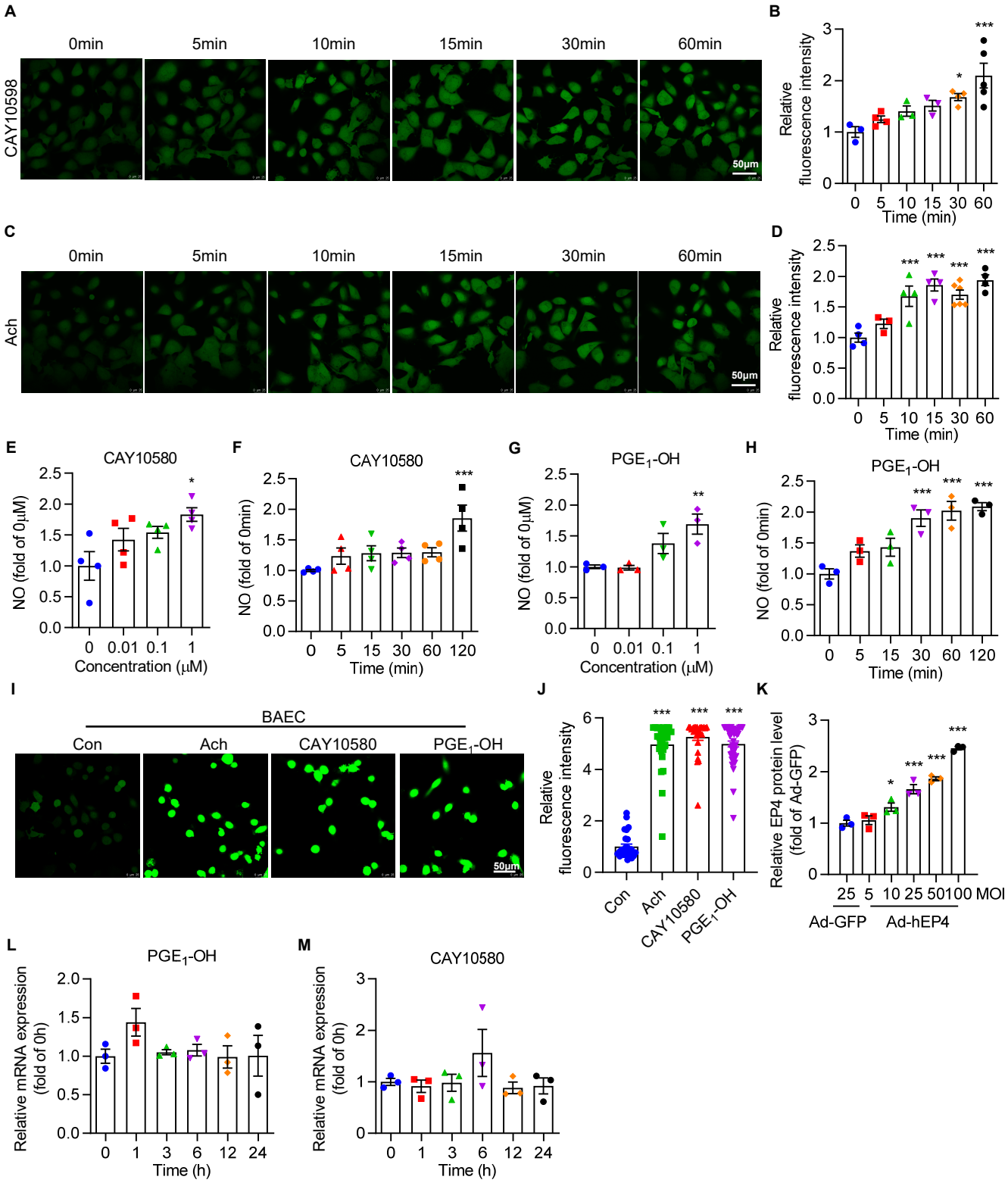

Figure S5. Effect of EP4 on NO production, eNOS phosphorylation and EP4 mRNA expression in cultured endothelial cells. (**A** and **B**) The time-course (A) and the relative fluorescence intensity (B) of NO production measured by DAF-FM DA in HUVECs treated with CAY10598. Scale bar: 50 μm. **p*<0.05, ****p*<0.001 *vs*.0 min, n=3-5. (**C** and **D**) The time-course (C) and the relative fluorescence intensity (D) of NO production as assessed by DAF-FM DA in HUVECs treated with Ach. Scale bar: 50 μm. ****p*<0.001 *vs*.0 min, n=3-6.

(**E** and **F**) The EP4 agonist CAY10580 increased NO production in HUVECs in a dose- (E) and time course-dependent manner (F).NO was measured by the Griess assay. *p<0.05 and ***p<0.001 *vs.*0 μM or 0 min, n=4. (**G** and **H**) The EP4 against PGE_1-OH increased NO production in HUVECs in a dose- (G) and time course-dependent manner (H). **p<0.01, ***p<0.001 *vs.* 0 μM or 0 min, n=3. (**I** and **J**) NO production measured by DAF-FM DA in BAECs treated with or without the EP4 agonist CAY10580 (1 μM) and PGE_1-OH (100 nM) for 30 min (I). Ach was used as a positive control. The relative fluorescence intensity in each group was compared (J). Scale bar: 50 μm. ***p<0.001 *vs.* control (Con), n=27-42. (**K**) Quantification of EP4 protein levels in Figure 5K. *p<0.05, ***p<0.001 *vs.* Ad-GFP, n=3. (**L** and **M**) Real-time PCR analysis showing that PGE_1-OH (L) and CAY10580 (M) treatment had little effect on eNOS mRNA expression in HUVECs. Data are represented as mean ± SEM, 1-way ANOVA followed by Dunnett's multiple comparisons tests are used.

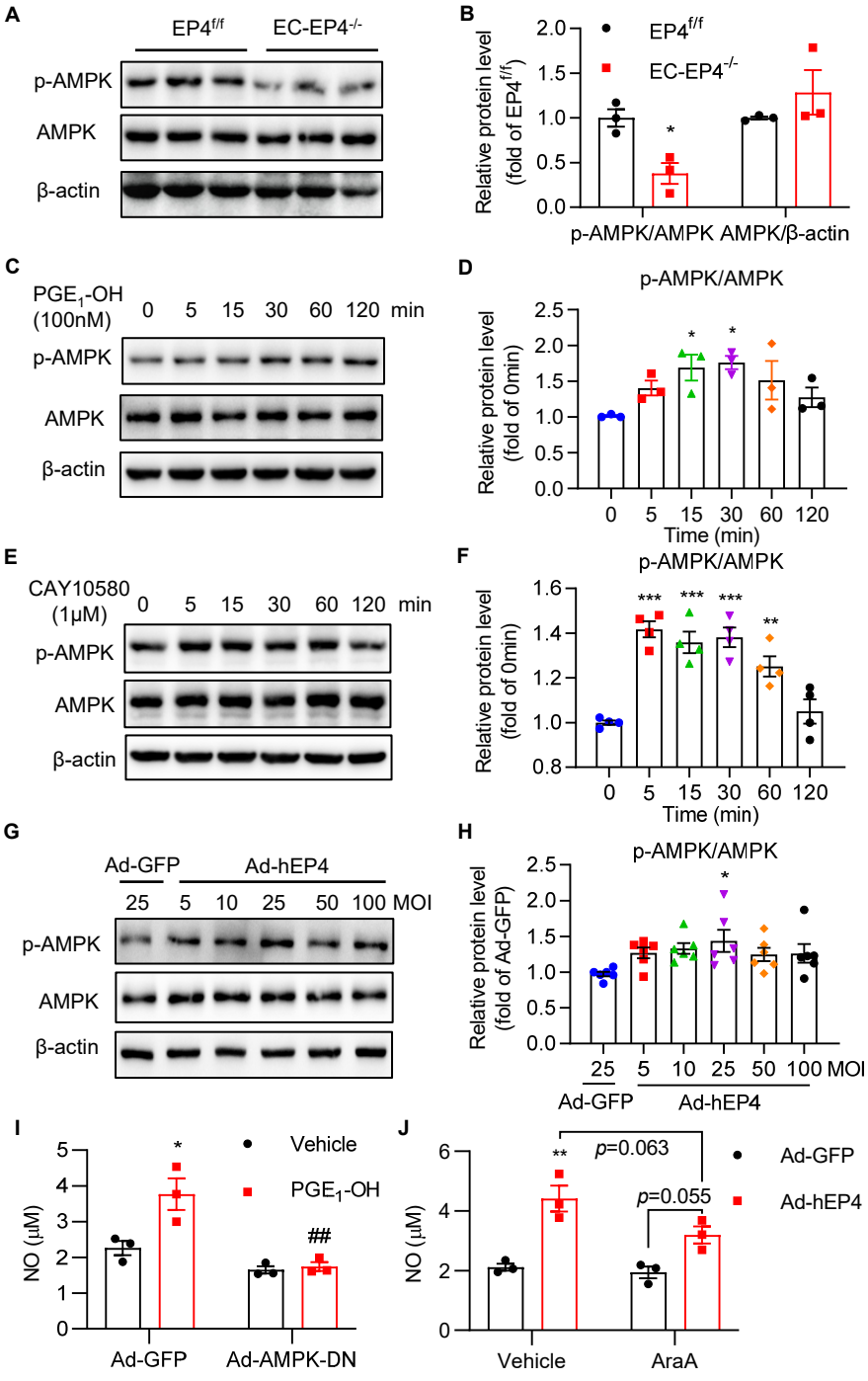

Figure S6. EP4 increases eNOS phosphorylation at Ser1177 via the AMPK pathway. (**A** and **B**) Western blot assay demonstrating that the protein levels of the phosphorylated AMPK in the mesenteric arteries of the EC-EP4$^{-/-}$ mice were significantly reduced compared to that in the EP4$^{f/f}$ mice (A). Protein quantification was performed by the Image J software (B). *p<0.05 *vs.* EP4$^{f/f}$, n=3. (**C** and **D**) Activation of EP4 by PGE$_1$-OH (100 nM) increased the phosphorylation of AMPK in a time-dependent manner in HUVECs as analyzed by western blot (C). Protein quantification was performed by using the Image J software (D). *p<0.05 *vs.* 0 min, n=3. (**E** and **F**) The time course of the effect of CAY10580 (1μM)-mediated EP4 activation on AMPK phosphorylation in HUVECs as analyzed by western blot (E). Quantification of protein level was performed by the Image J software (F). **p<0.01, ***p<0.001 *vs.* 0 min, n=3. (**G** and **H**) Adenovirus-mediated EP4 overexpression increased the p-AMPK levels in a dose-dependent manner in HUVECs (G). The cells were infected with

the adenoviruses for 36 hours. Protein levels were quantified by the Image J software (H). *p<0.05 *vs.* Ad-GFP, n=3. (**I**) Suppression of AMPK activity via an adenovirus-mediated overexpression of a dominant negative AMPK construct (Ad-AMPK-DN) blocked PGE_1-OH-induced NO production in HUVECs. *p<0.05 *vs.* vehicle, ##p<0.01 *vs.* Ad-GFP+PGE_1-OH, n=3. (**J**) The AMPK inhibitor AraA reduced Ad-EP4-induced NO production in HUVECs. **p<0.01 *vs.* Ad-GFP, n=3. Data are represented as mean ± SEM, 2-way ANOVA followed by Sidak's multiple comparisons test for **B**; 1-way ANOVA followed by Dunnett's multiple comparisons tests for **D**, **F** and **H**; 2-way ANOVA followed by Tukey's multiple comparisons tests for **I** and **J**.

Table S1. Cardiac function-related parameters were not different between the $EP4^{f/f}$ and $EC\text{-}EP4^{-/-}$ mice.

Parameters	$EP4^{f/f}$	$EC\text{-}EP4^{-/-}$
LVAW;d (mm)	0.933±0.025	0.993±0.227
LVAW;s (mm)	1.380±0.124	1.435±0.258
LVID;d (mm)	4.417±0.259	4.194±0.405
LVID;s (mm)	3.294±0.476	2.979±0.388
LVPW;d (mm)	0.880±0.248	0.747±0.106
LVPW;s (mm)	1.155±0.282	1.080±0.167
Ejection fraction (%)	50.28±10.83	56.30±4.510
Fractional Shortening (%)	25.80±6.943	29.18±2.757
LV Mass (mg)	130.6±14.27	113.1±13.15
LV Vol;d (μL)	88.95±12.07	79.40±17.47
LV Vol;s (μL)	45.39±14.74	35.36±10.99
Stroke Volume (μL)	43.56±4.750	44.03±7.180
Cardiac output (mL/min)	20.89±2.442	20.78±3.282
Heart rate (BPM)	479.6±11.97	471.8±4.310

Table S2. Cardiac function-related parameters were not different between the LSL-hEP4$^{f/f}$ and EC-hEP4^{OE} mice.

Parameters	LSL-hEP4$^{f/f}$	EC-hEP4^{OE}
LVAW;d (mm)	0.889±0.146	0.860±0.120
LVAW;s (mm)	1.240±0.183	1.322±0.166
LVID;d (mm)	3.901±0.193	4.032±0.218
LVID;s (mm)	2.891±0.236	3.091±0.166
LVPW;d (mm)	0.775±0.046	0.900±0.191
LVPW;s (mm)	1.069±0.086	1.167±0.205
Ejection fraction (%)	51.53±5.069	47.05±4.212
Fractional Shortening (%)	25.98±3.142	23.29±2.515
LV Mass (mg)	95.01±7.995	108.1±10.18
LV Vol;d (μL)	66.20±7.629	71.66±9.233
LV Vol;s (μL)	32.33±6.262	37.83±5.042
Stroke Volume (μL)	33.88±3.234	33.82±5.781
Cardiac output (mL/min)	16.12±1.623	16.13±2.760
Heart rate (BPM)	475.8±6.765	477.0±0.632

Table S3. Primers used for real-time PCR.

Gene Name	Forward primer sequence (5′-3′)	Reverse primer sequence (5′-3′)
Mouse EP1	TAACGATGGTCACGCGATGG	ATGCAGTAGTGGGCTTAGGG
Mouse EP2	ATGCTCCTGCTGCTTATCGT	AGGGCCTCTTAGGCTACTGC
Mouse EP3	GGATCATGTGTGTGCTGTCC	GCAGAACTTCCGAAGAAGGA
Mouse EP4	ATGGTCATCTTACTCATCGCCAC	CCTTCACCACGTTTGGCTGAT
Mouse β-actin	CCCTGGAGAAGAGCTACGAG	CGTACAGGTCTTTGCGGATG
Human eNOS	CAACGCTACCACGAGGACATT	CTCCTGCAAAGAAAAGCTCTGG
Human β-actin	CTCCATCCTGGCCTCGCTGT	GCTGTCACCTTCACCGTTCC

The annealing temperature was 59℃ for all genes examined.

Table S4. Primers used for genotyping.

Gene Name	Primer sequence (5′-3′)	Products length (bp)	Annealing temperature
EP4 genotyping (P1 and P2)	F: GGAGTCACTTTTCCCTTGAGAAG R: AGCGAGTCCTTAGGCTTTTAAGT	370(KO) 1811(WT)	59℃
Flox genotyping (P3 and P4)	F: TCTGTGAAGCGAGTCCTTAGGCT R: CGCACTCTCTCTCTCCCAGGAA	243(WT) 344(flox)	60℃
Tie2-Cre genotyping	F: ACCTGAAGATGTTCGCGATTATCT R: ACCGTCAGTACGTGAGATATCTT	370	60℃
LSL-hEP4-flox genotyping	F: GGGCAGTCTGGTACTTCCAAGCT R^{WT}: ATATCCCCTTGTTCCCTTTCTGC R^{flox}: TGGCGTTACTATGGGAACATACGTC	268(WT) 335(flox)	55℃